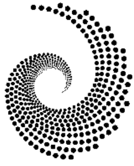

COMPUTATIONAL RESEARCH PROGRESS IN APPLIED SCIENCE & ENGINEERING (CRPASE)

CRPASE: TRANSACTIONS OF MECHANICAL ENGINEERING

Journal homepage: http://www.crpase.com

CRPASE: Transactions of Mechanical Engineering, Vol. 06(04), 281-287, December 2020 ISSN 2423-4591

Research Article

Comparative Study of Physics of Failure Assessments of Thermomechanical Fatigue for Solder Joints in Multichip Module Under Different Conditions

Cheng-Geng Huang*

School of Intelligent Systems Engineering, Sun Yat-sen University, China

Keywords

Thermo-mechanical reliability,
Creep-fatigue failure,
Qualification tests,
Solder joints,
Multi-chip module.

Abstract

A multi-chip module (MCM) which is integrated by multiple integrated circuits (IC) into a unified substrate can significantly reduce the interconnection spacing between various chips and enhance the electrical characteristics. Despite multi-chip module's greater performance compared with traditional encapsulation, the corresponding problem is mainly induced by thermo-mechanical, and the reliability assessment has also been a critical issue in the electronic industry. The creep-fatigue failure of solder joints under cyclic temperature fluctuations, which is caused by both ambient temperature changes and internal power cycling, plays an important role in the thermo-mechanical reliability of the MCM. In order to assess the influence of cyclic temperature loading profiles on the fatigue life of the solder joints, three different kinds of temperature-related qualification tests, i.e. accelerated temperature cycles (ATC), thermal shock cycles and modified temperature cycles with 10-minutes dwell period, are utilized in the finite element analysis (FEA). Using the FEA method, we can obtain the critical solder joints located in the outer corner of the substrate in MCM and the specific failure location of the solder joint, which is validated by the optical micrograph. Furthermore, based on the energy-partitioning damage model, a comparative analysis of the fatigue life of critical solder joints under various temperature loading profiles is made. The results obtained can improve the design and manufacture in the field of microelectronics encapsulation. For a basic qualification test, these results can also provide the guidelines for the engineers and manufacturers.

1. Introduction

At the present, the microelectronics encapsulation is making an effort towards lighter, thinner, better cost-performance and becomes much more reliable. As one of the state of the art encapsulation, MCM has been widely used in the field of military and aerospace to automotive, industrial equipment, medical facility, and electronic system products. MCM has a greater package density and power density, resulting in the greater thermal and stress or strain should be a major concern for thermo-mechanical reliability. The solder joints provide the electrical, thermal and mechanical interconnect between the substrate and the printed wiring board (PWB) of the MCM. The fatigue failure of solder joints caused by alternating mismatches in the coefficient of thermal expansion (CTE) among the substrate and PWB of the MCM plays a dominant role in the failure modes of the MCM. Due to the time-temperature dependent creep and plastic behaviors of the Sn-Ag-Cu (SAC) in solder joints, fatigue life prediction of solder joints under thermal cyclic loadings still remains a difficult subject [1].

As microelectronics encapsulation should meet the requirements of specific quality and reliability for application, MCM must undergo a process of qualification to assess its quality and reliability [2]. Compared with the conventional life tests for MCM, accelerated life test is much more economical and practical. The temperature excursion can also influence the life of electronic package, which is

* Corresponding Author: Cheng-Geng Huang
E-mail address: Cheng-geng.huang@hotmail.com

Received: 19 September 2020; Revised: 18 October 2020; Accepted: 22 October 2020

Please cite this article as: Ch. G. Huang, Comparative Study of Physics of Failure Assessments of Thermomechanical Fatigue for Solder Joints in Multichip Module Under Different Conditions, Computational Research Progress in Applied Science & Engineering, CRPASE: Transactions of Mechanical Engineering 6 (2020) 281–287.

known as the "10ºC rule" [3]. The reliability tests for electronic packages are often employed in temperature test that is accelerated temperature cycles (ATC) or thermal shock cycles. Based on the load specifications of IPC 9701 [4], three different temperature load profiles are used to comprehensively analyze the influence of temperature fluctuation on fatigue damage and fatigue life of the solder joints in MCM.

Creep deformation of the SAC solder joints becomes much more significant, since the solder joints in MCM are usually subjected to the stress at a high temperature which is above the homologous temperature of 0.4 [5]. Under reliability testing and operating conditions, the solder joints are prone to creep-fatigue failure related to the mechanisms of damage due to the combined effects of creep and fatigue. Based on the continuum damage mechanics theories, several creep-fatigue models have been developed to predict the fatigue life of solder joints in MCM. Wong [6] presented a review of these creep fatigue models by the means of compounding damage caused by creep and fatigue mechanisms, and also made an effort to divid these models into eight categories. Among these models, strain energy-partitioning damage model [1] was employed to calculate fatigue life of solder joints under the different temperature loading profiles.

Furthermore, in order to investigate the influence of the ramp rate of temperature and the condition of dwell time period on the damage evolution of the critical solder joints, comparative evolutions of the accumulated equivalent plastic and creep strain in critical solder joints were obtained. According to the common procedures, the elastic, plastic and creep strain energy densities are averaged over 10% of the solder joint volume which lies in the vicinity of the most critical region of the joint. The results show that the ramp rate of temperature and the condition of dwell time period has a negligible effect on the elastic strain energy density of the 10% averaged volume. However, the accumulated equivalent creep energy density, with ladder-like distribution characteristics during temperature loading profiles, is mainly influenced during the dwell time period. In contrast, the accumulated equivalent plastic energy density gradually increases as the elevated ramp rate of the temperature and still remains stable during the dwell time period. The content of this paper is attached to the virtual qualification that is the first stage of the overall qualification process [2], and the results obtained can contribute to the qualification guidelines of the MCM for designers and manufacturers.

2. Thermal Stress and Strain Analysis for the MCM under Different Temperature Cycles

2.1. FEA Model of the MCM

During ATC and thermal shock, thermal induced stress and strain are the dominant factors for the failure of the MCM. In order to realize the critical zone which has the highest stress and strain and make further analysis about the fatigue life of the MCM, the FEA model of the MCM developed using ANSYS 14.5TM [7] will be discussed in details in this section.

Because of the perfectly symmetrical characteristic of the MCM, eight-node pure hexahedral elements are used in this simulation. The lower-left part of the Figure 1 (in Appendix) presents the meshed model of the quarter section of MCM architecture. To clearly demonstrate the details of the package, meshed submodels of the MCM are also encompassed in Figure 1, and the relevant geometric dimensions are shown in Table 1. In Figure 1, there are three dies with the corresponding die attaches integrating into a unifying substrate, and the dies mapped for magenta are enclosed by the overmold. As the overmold has non-geometric characteristics, the detailed information about the length and the width is not given in Table 1 (N means unavailable details). The material properties except solder joint are summarized in Table 2, including Young's modulus, Poisson's ratio, and coefficient of thermal expansion. The substrate and the PWB are modeled as transversely isotropic materials.

Table 1. Geometric package dimensions for MCM

Dimensions	*Length (mm)*	*Width (mm)*	*Height (mm)*
Overmold	N	N	0.595
Die1	5	4	0.51
Die attach1	5	4	0.07
Die2/Die3	4	4	0.51
Die attach2/ Die attach3	4	4	0.07
substrate	17.5	17.5	0.513
PWB	38.5	38.5	1.47
Dimensions of a unit of the solder joint			
Dimensions	*Diameter (mm)*	*Height (mm)*	*Pitch (mm)*
Top Cu pad	0.254	0.032	1
Bottom Cu pad	0.225	0.019	1
Solder joint	0.310	0.62	1
Solder neck	0.160	0.32	1

Due to the time-temperature dependent creep behavior, the time-dependent plastic behavior and the temperature-dependent elastic behavior of the Sn3.9Ag0.6Cu solder (SAC396), a partitioned constitutive relationship for elastic, plastic and creep properties are adopted in material properties modelling of solder. Based on the results from the thermos-mechanical-microscale (TMM) tests conducted by Zhang [8], solder elastic and plastic properties are given in Table 3.

Rate-independent plastic property of the solder is typically modeled with a power-law function, that is,

$$\begin{aligned} &\tau = C_{pl}\gamma_{pl}{}^{n}, \\ &C_{pl} = 60.1 - 0.18 * T(^{\circ}\mathrm{C}), \\ &n = 0.29 - 0.00046 * T(^{\circ}\mathrm{C}) \end{aligned} \tag{1}$$

where τ, γ_{pl} are the shear stress and the plastic strain, respectively; C_{pl}, n are the temperature-dependent material constants.

Time-temperature dependent creep property is modeled with a Garafalo hyperbolic sine model to describe its secondary (steady-state) creep strain rate [9], and the form of the creep strain rate is shown as follows:

$$\dot{\varepsilon}_{cr} = A \times [\sinh(\lambda\sigma)]^{n} \times \exp(-\frac{Q}{R \times T(K)}) \tag{2}$$

where A and n are the material constants; λ is associated with the stress level at which the power-law dependence breaks down; Q, R and T are the activation energy, universal gas constant and absolute temperature, respectively.

Due to symmetrical characteristic of the MCM, only the quarter section of MCM is modeled in ANSYS APDL. The symmetry displacement boundary constraints are put on the planes of the symmetry, and the constraint in all directions are then put on the origin node of the model. According to the load specifications of IPC 9701 [4], the accelerated temperature cycles, thermal shock cycles and modified accelerated temperature cycles with 10-minute dwell time at peak temperature levels are adopted in the finite element simulation. The detailed temperature load profiles are presented in Figure 2, and the corresponding qualification test conditions for surface mount solder attachments are summarized in Table 4. And the detailed information about the load steps for each test environments used in ANSYS APDL are presented in Table 5 (in Appdenix).

Table 2. Linear elastic material properties for MCM

Material properties	E(GPa)	v	$CTE(ppm/°C)$
Overmold	23.6	0.30	9
Silicon die	19.1	0.278	2.1
Die attach	1.2	0.42	110
Substrate (BT)	20 (X, Z)	0.11 (XZ)	15 (X, Z)
	4 (Y)	0.39 (XY, YZ)	60 (Y)
Solder pad(Copper)	12.9	0.35	19
PWB (FR4)	17.685 (X, Z)	0.11 (XZ)	18 (X, Z)
	7.709 (Y)	0.28 (XY, YZ)	60 (Y)

Table 3. Partitioned constitutive properties for SAC396

Elastic [8]	E(GPa) 18.6-0.021T (oC) [8]		v 0.35	CTE(ppm/oC) 26
Plastic [8]	Cpl (Mpa) 60.1-0.18*T (oC)		n 0.29-0.00046*T (oC) [8]	
Steady-State Creep [9]	A 0.0271	λ (1/Mpa) 0.369	n 1.05	Q (J/mol) 5.1E+3

Table 4. Qualification test conditions for surface mount solder attachments [4]

Test environments	Temperature cycle (oC)	Ramp rate (oC /min)	Dwell time period (min)
ATC	-55/125	10	
TS	-55/125	25	
MATC	-55/125	10	10

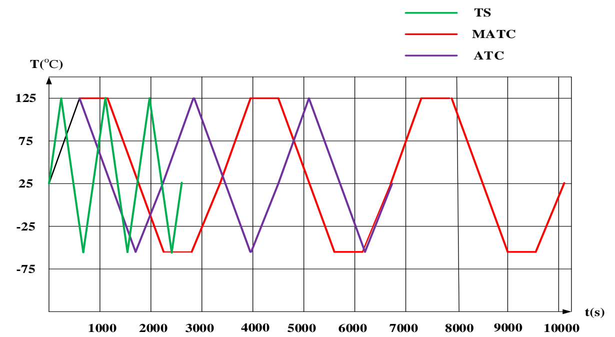

Figure 2. Temperature load profiles for simulation of solder joint in MCM

2.2. Thermal Stress and Strain for the MCM under MATC Profile

For the analysis of thermal induced stress and strain contours, it is found that the entire distributions of equivalent stress and strain tend to be similar to each other under three different temperature load profiles. Here, only the stress contours of each encapsulation parts excluding the solder joints in MCM at the end of the third cycle under the condition of MATC are given in Figure 3. It is observed that the equivalent stress distribution in PWB, substrate, die, die attach and overmold are almost uniform and less than 10Mpa. It is worth noting that the maximum equivalent stress occurs at corner solder pad and equals to 89.8692Mpa, yet the corresponding equivalent strain only remains a relatively minimum amount of 0.697×10^{-3} percent due to the higher stiffness of solder pad.

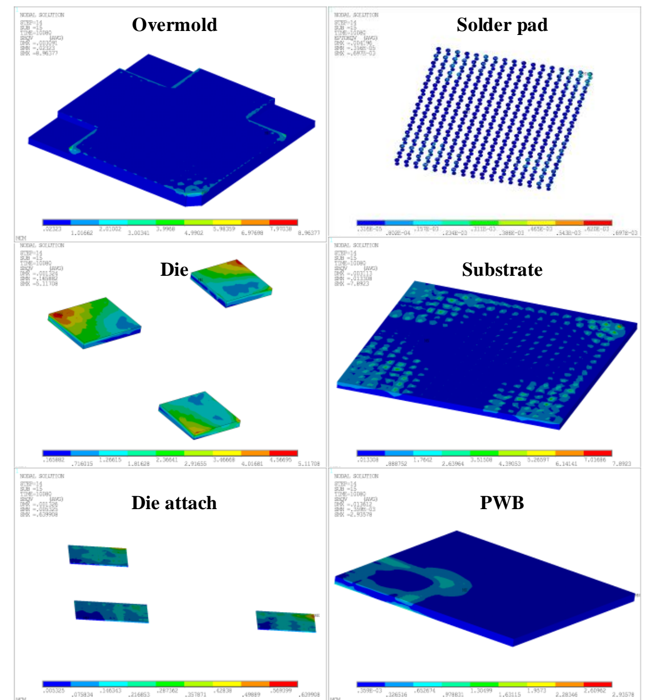

Figure 3. Stress contours of each encapsulation parts in MCM

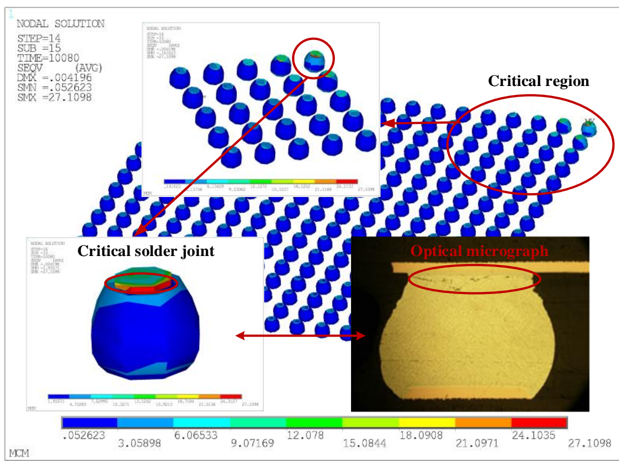

Figure 4. Stress contours of the critical solder joint of MCM and the typical optical micrograph of the corresponding solder joint, indicating crack initiation [11]

Figure 4 illustrates the equivalent stress contours of solder joints at the end of the third cycle under the condition of MATC. It is found that the critical regions of MCM always appear in the outermost corner with the maximum distance from neutral point (DNP) of the grid array of solder joints [10]. Due to the stress concentration, the highest equivalent stress and strain are found in the solder neck known as the solder/IMC interface, where the micro cracks and cavities initiate and propagate up to the eventual failure of the solder joint, resulting in the catastrophic failure of MCM. The equivalent stress is equal to 27.1098Mpa and the corresponding equivalent strain reaches a maximum of 0.055398 percent. The reason might be attributed to the coefficient of thermal expansion mismatch between the substrate and the PWB of the MCM. Moreover, the stress contours of the critical solder joints are correctly validated by the optical micrograph of the corresponding solder joint which is consistently located in the outmost corner of the grid array of solder joints.

3. Comparative Study of Response and Life Prediction of the Critical Solder Joint in MCM under Different Loading Profiles

It has been widely accepted that the energy partition method proposed by dasgupta et al. [1] is applicable to model the creep-fatigue of solder joints in microelectronic assembly [12-13]. Energy partition model is used to formulate the elastic strain-energy stored, plastic energy dissipation Wp and creep energy dissipation Wc per cycle for accurately predicting the number of thermal cycles to failure of the critical solder joint. The cyclic elastic strain-energy density (Ue) is estimated by the FEA results. As the evolution of Ue is roughly consistent under different loading profiles, Figure 5 only describes the evolution of Ue at the critical element in the critical solder joint under the condition of MATC. Further, it can be concluded that Ue can be negligible (only equals to about 0.013mJ/mm3) at the end of the third temperature cycle, so this energy-partition model only takes Wp and Wc into account to calculate the fatigue life cycles of the solder joints in MCM.

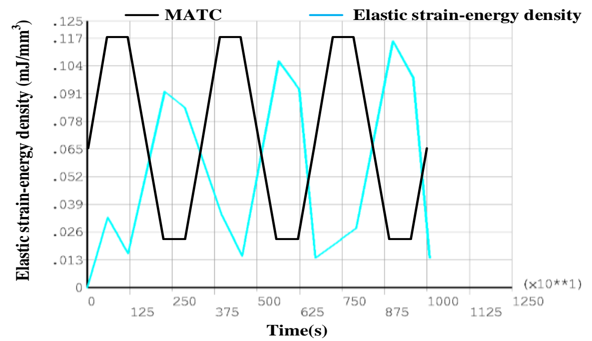

Figure 5. Evolution of Ue at the critical element in critical solder joint for MATC

The energy partition damage model (E-P model), only accounting for plastic energy dissipation and creep energy dissipation, can then be expressed as

$$Energy = W_p + W_c = W_{po}(N_{fp})^{c'} + W_{co}(N_{fc})^{d'} \quad (3)$$

where c', d' are the slopes; *Wpo* and *Wco* are the corresponding intercepts of the plots of *Wp* and *Wc* versus cycles to failure on a log-log scale, respectively. N_{fp} and N_{fc} are the thermal cycles to failure responsible for the plastic energy dissipation and creep energy dissipation, respectively. As the E-P model constants for Sn3.9Ag0.6Cu are expected to be similar to those of Sn3.8Ag0.7Cu, these constants can be obtained from Zhang et al. [14], as shown in Table 6.

Table 6. E-P model constants for Sn3.8Ag0.7Cu [14]

E-P model of Sn3.8Ag0.7Cu [14]	c'	d'	*Wpo* *(mJ/mm³)*	*Wco* *(mJ/mm³)*
	-0.8	-1.4	198	1.23E4

Further, using Miner's linear damage rule, the estimated fatigue life for critical solder joint can be given as

$$Damage = \frac{1}{N_f} = \frac{1}{N_{fp}} + \frac{1}{N_{fc}} \quad (4)$$

In order to minimize the effect of the mesh density on the energy partition constants, plastic and creep energy density per cycle are the average value of some elements, which enclose 10% of the critical solder joint volume in the critical region [14], i.e. solder neck, as shown in Figure 6.

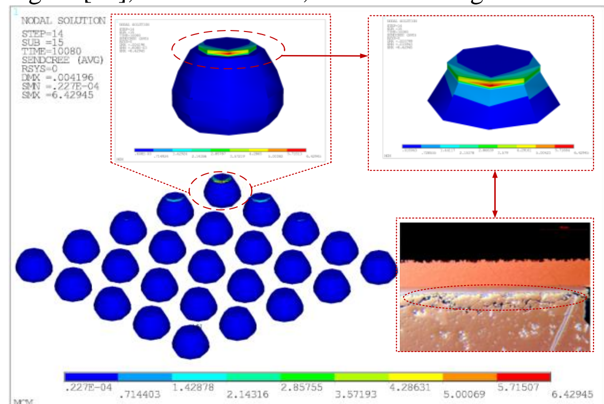

Figure 6. Highlight of the critical element, 10% of the critical solder joint volume for MATC and its corresponding optical micrograph

The accumulated plastic and creep work densities can be viewed as a damage indicator to present the fatigue process of solder joints. Comparative evolutions of plastic and creep work densities in the 10% of the critical solder joint volume in the critical region when subjected to the different temperature profiles, i.e. ATC, TS and MATC, are presented in Figure 7. In the Figure, the accumulated equivalent creep and plastic work densities are *Wcr* and *Wpl*, respectively.

The larger magnitude of *Wcr* subjected to MATC is achieved when compared with ATC and TS primarily due to the effect of 10-min dwell time. By contrast, the dwell time has a slight effect on *Wpl*. And the lower ramp rate of temperature could induce the greater *Wcr*, as shown in Figure 7. Moreover, the cumulative increase of accumulated equivalent creep and plastic work density has a ladder pattern till the catastrophic fracture failure of the solder joint. Comparing with *Wcr*, *Wpl* is greatly influenced by the ramp rate of temperature. Thus, the damage induced by the profile of MATC should be greater than that of ATC and TS. Consequently, the fatigue life cycle with MATC profile is much shorter than the other two profiles. More investigations should also be made about the evolution of *Wcr* and *Wpl* with MATC profiles.

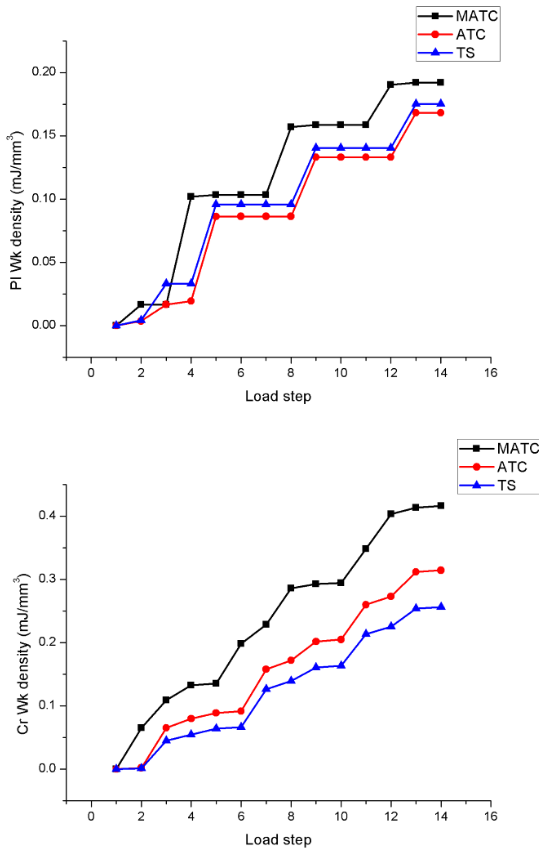

Figure 7. Comparative evolutions of Wcr and Wpl versus load steps under the temperature profiles of ATC, TS and MATC

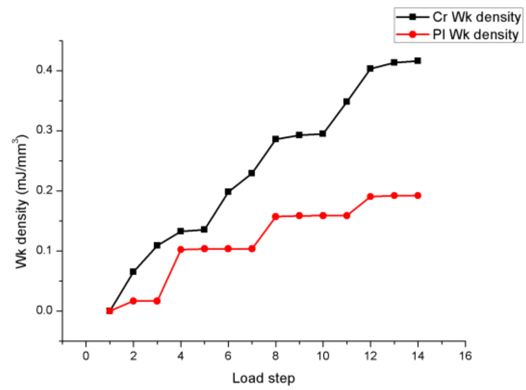

Figure 8. Evolutions of Wcr and Wpl versus load steps under the temperature profile of MATC

As shown in Figure 8, the curve of Wcr is much steeper than that of Wpl during the MATC profile, the effect of creep plays a dominant role of the critical solder joint failure. It is noteworthy that the nominal slope of the curves is different for each load step that the specific influence of dwell time as well as the ramp rate of temperature remains complicated.

As shown Figure 9, compared with the dwell time period at lowest temperature, the dwell time period at highest temperature has a significant influence on Wcr. This could be attributed to that the high temperature (homologous temperature: T/Tm>0.5) accelerates the effect of creep. Besides, the process of temperature rise and temperature drop has a great effect on Wcr. By contrast, the dwell time period has little impact on Wpl as shown in Figure 9. In addition, Wpl is mainly affected by the process of temperature drop.

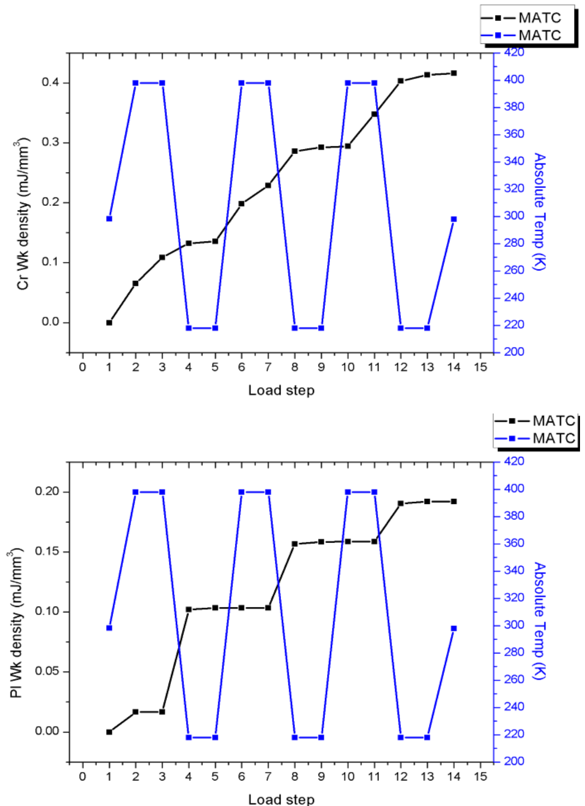

Figure 9. Evolutions of Wcr and Wpl versus load steps and the specific temperature profile of MATC

According to the customary procedures proposed by Dasgupta et al. [1], the value of Wcr and Wpl per cycle in the 10% of the critical solder joint volume in the critical region is calculated by using the general postprocessor of ANSYS APDL. Based on the E-P model, the cycles to failure caused by creep and plastic work dissipation, i.e. Nfc and Nfp, can be obtained. Further, using Miner's linear damage rule, the prediction of failure life for critical solder joint in MCM under different temperature profiles can be achieved. The corresponding results are shown in Table 7.

Table 7. Comparison of cycles to failure (Nf) of the critical solder joint under different temperature profiles

Temp profiles	MATC	ATC	TS
Wcr *(mJ/mm³)*	157.1×10^{-3}	92.2×10^{-3}	84.7×10^{-3}
Wpl *(mJ/mm³)*	55.1×10^{-3}	67×10^{-3}	62.5×10^{-3}
Nfc	3130	4580	4866
Nfp	27822	21789	23767
Cycles to failure (*Nf*)	2814	3785	4039

From Table 7, the cycles to failure of the critical solder joint under MATC profile is equal to 2814, which is the minimum cycles to failure, compared with the other two profiles. Hence, the dwell time period has a significant influence on the fatigue life of the critical solder joint, because the dwell time period accelerates the creep effect. In addition, the cycles to failure of the critical solder joint under ATC and TS profiles remain the same. So the ramp temperature rate has less effect on the fatigue life of the critical solder joint.

4. Conclusions

Due to the symmetrical characteristic of the MCM, only the quarter section of MCM is modeled in ANSYS APDL. The corresponding boundary constraints are put on the model, and the load specifications of IPC 9701 are adopted in the simulation. It is found that the critical region situated in solder joint with the maximum DNP under three different temperature profiles. The highest equivalent stress and strain are found in the solder neck known as the solder/IMC interface, which is validated by the optical micrograph of the corresponding solder joint.

Based on the energy damage model (E-P model), the cyclic elastic strain-energy density (Ue) is found to be negligible. Besides, following the customary procedure to eliminate the effect of the mesh density, 10% of the critical solder joint volume in the critical region is used to comparatively assess the response and fatigue life of the critical solder joint in MCM under different loading profiles. In this study, the following conclusions can be made.

1. The dwell time period has a prominent influence on the accumulated equivalent creep work densities (Wcr). And the lower ramp rate of temperature can induce the greater Wcr. The accumulated equivalent creep and plastic work densities (Wcr and Wpl) has a ladder pattern distribution.
2. As for the evolution of Wcr and Wpl with MATC profile, Wcr is much steeper than that of Wpl during the MATC profile, and thus the effect of creep plays a dominant role of the critical solder joint failure.
3. The dwell time period at the highest temperature has a significant influence on Wcr. However, it has little effect on Wpl which is mainly affected by the process of temperature drop. In addition, both the processes of temperature rise and temperature drop have great effect on Wcr.
4. The dwell time period has a significant influence on the fatigue life of the critical solder joint. And the ramp temperature rate has less effect on the fatigue life of the critical solder joint.

Conflict of Interest Statement

The authors declare no conflict of interest.

References

[1] A. Dasgupta, C. Oyan, D. Barker et al., Solder creep-fatigue analysis by an energy-partitioning approach, Journal of electronic packaging 114 (1992) 152–160.

[2] H. Ardebili, M. Pecht, Encapsulation technologies for electronic applications. USA: William Andrew, 2009.

[3] Kin. Yoshinori and Sasaki. Yasuko, What is Environmental Testing?, ESPEC Technology Report (1996) 2–16.

[4] IPC 9701: Performance Test Methods and Qualification Requirements for Surface Mount Solder Attachments. Association Connecting Electronics Industries (IPC).

[5] M. N. Tamin, N. M. Shaffiar, Solder joint reliability assessment: Finite Element Simulation Methodology. Berlin: Springer series, 2014.

[6] E. H. Wong, W. D. van Driel, A. Dasgupta, et al, Creep fatigue models of solder joints: a critical review, Microelectronics Reliability 59 (2016) 1–12.

[7] ANSYS 14.5, ANSYS INC, available at: http://www.ansys.com/.

[8] Q. Zhang, A. Dasgupta, and P. Haswell, Partitioned Viscoplastic-Constitutive Properties of the Pb-Free Sn3.9Ag0.6Cu Solder, TMS Journal of Electronic Materials 33, (2004) 1338–1349.

[9] G. Cuddalorepatta and A. Dasgupta, "Viscoplastic Behavior of Hypo-Eutectic Sn3.0ag0.5cu Pb-Free Alloy Under Creep Loading Conditions, ASME 2007 International Mechanical Engineering Congress and Exposition (2007)159–167.

[10] R. Ghaffarian, N. P. Kim, "Ball grid array reliability assessment for aerospace applications, Microelectronics Reliability 39 (1999) 107–112.

[11] J. Johansson, I. Belov, E. Johnson, et al, Investigation on thermal fatigue of SnAgCu, Sn100C, and SnPbAg solder joints in varying temperature environments, Microelectronics Reliability 54 (2014) 2523–2535.

[12] E. H. Wong, Y. W. Mai, A unified equation for creep-fatigue, International Journal of Fatigue, 68, (2014) 186-194.

[13] K. C. Kapur, M. Pecht, Reliability engineering. USA: John Wiley & Sons, 2014.

[14] Q. Zhang, Isothermal mechanical and thermo-mechanical durability characterization of selected Pb-free solders. Ph.D. Dissertation, University of Maryland, 2004.

Appendix.

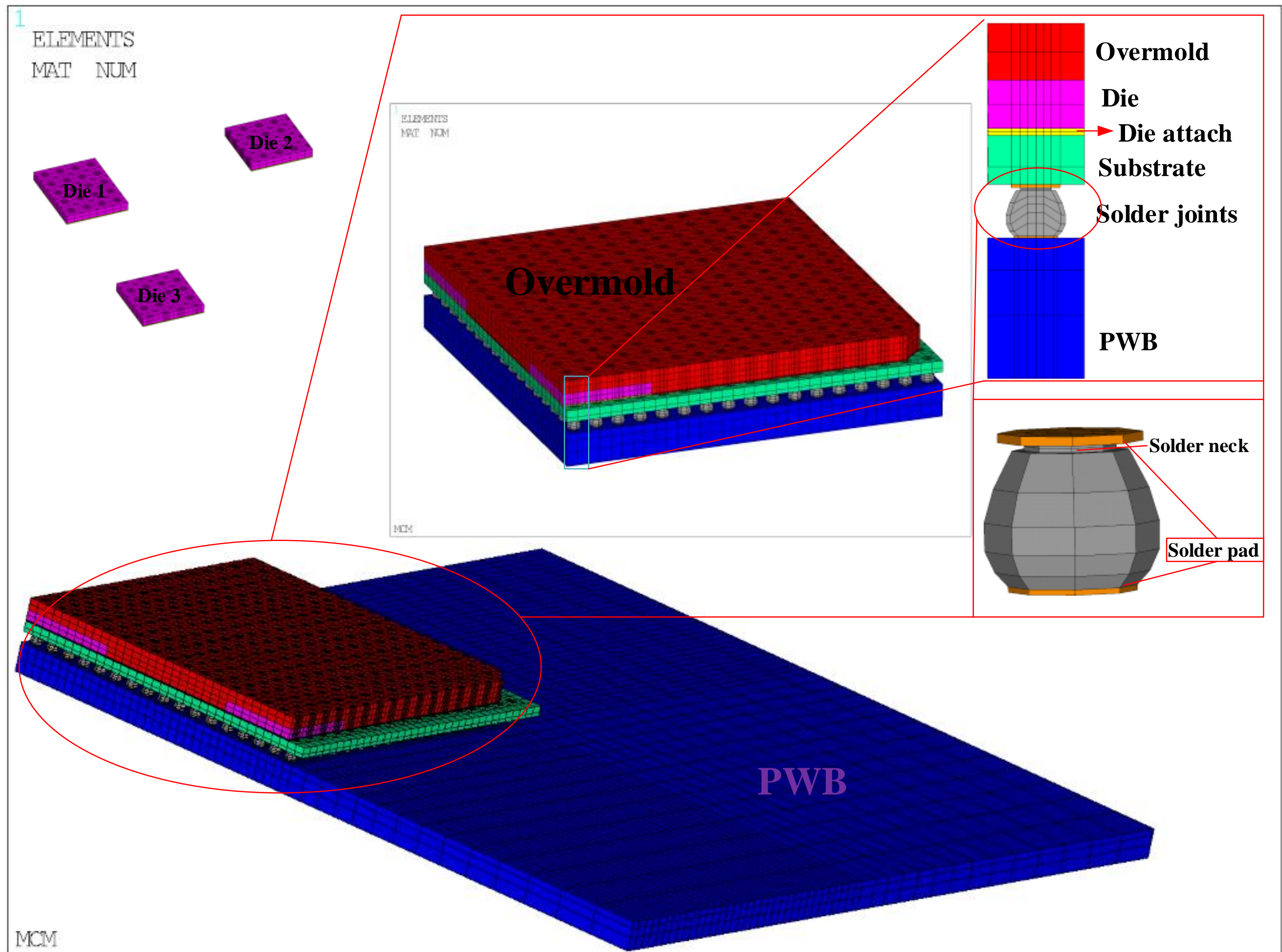

Figure 1. Finite element model of MCM

Table 5. Detailed information about the load steps for ATC, TS and MATC

Test Conditions / Load Steps	ATC		TS		MATC	
	Temp(°C)	Time(s)	Temp(°C)	Time(s)	Temp(°C)	Time(s)
LS1	25.16	1	25.5	1	25.16	1
LS2	75	300	75	120	125	600
LS3	125	600	125	240	125	1200
LS4	25	1200	45	432	-55	2280
LS5	-55	1680	-55	672	-55	2880
LS6	45	2280	45	912	125	3960
LS7	125	2760	125	1104	125	4560
LS8	25	3360	25	1344	-55	5640
LS9	-55	3840	-55	1536	-55	6240
LS10	45	4440	45	1776	25	6720
LS11	125	4920	125	1968	125	7920
LS12	25	5520	25	2208	-55	9000
LS13	-55	6000	-55	2400	-55	9600
LS14	25	6480	25	2592	25	10080